DETAILED MAGELLAN RADAR REFLECTIVITY VARIATIONS WITHIN SUDENITSA TESSERA, VENUS. I. Ganesh[1] and M. S. Gilmore[2], [1]Geophysical Institute, University of Alaska Fairbanks, AK (iganesh@laska.edu), [2] Dept. of Earth and Environmental Sciences, Wesleyan University, CT.

Introduction: About 7–8% of Venus's surface is covered by highly deformed and structurally complex terrain called tesserae [1]. Based on embayment and superposition relationships between the tesserae and the globally prevalent volcanic plains, and crater retention studies, the tesserae are hypothesized to be the oldest units of Venus's surface, with an estimated age of 1 to .4X the average surface crater retention age of 300 - 1000 Ma [2,3]. Variations in surface age, formation mechanisms, lithology and composition, and geologic evolution at both inter- and intra-tessera scales are not well-understood and continue to remain the focus of numerous studies and future spacecraft missions [4,5].

Recent workers have focused on identifying regions of allochthonous sediments within the tesserae, to assist future missions with selecting sampling sites that represent true tessera composition (i.e., uncontaminated by plains material). These studies made use of Arecibo synthetic-aperture radar (SAR) polarimetry data [6] and Magellan SAR backscatter data [7] to map regions within tesserae that are likely covered by distal, fine-grained lofted impact ejecta (crater parabola deposits) associated with (both observed and erased) craters on Venus. Identifying and characterizing areas of sediments, whether allochthonous or locally derived, within tesserae has broad-ranging implications for surface ages, erosion rates, composition and geologic timeline of events occurring within tesserae.

Here we introduce an approach that uses Magellan SAR backscatter and nadir surface reflectivity datasets together, to explore inter- and intra-tesserae variability, with a specific focus on identifying sites of fine-grained mantling material. We investigate tessera terrain across the planet to reevaluate previously proposed sites of sediments on tesserae, and identify additional potential sites of sediment-mantling.

Data and methods: The Magellan mission to Venus acquired information about the surface using side-looking SAR imaging and nadir-pointing altimeter. In this study, we use

1. HH-polarized backscatter from left-looking SAR FMAPS (~100 m/px resolution) [8], and
2. nadir surface reflectivity obtained from the altimeter as recorded by the Altimetry and Radiometry Composite Records (ARCDR) [9].

We extract all the ARCDR footprints that fall within tessera terrain and are at least 10 km away from the boundaries (to discard any footprints that might contain information from both tesserae and adjacent plains). We then select only those footprints over areas for which SAR data is available. The SAR data are then used to (1) apply a SAR backscatter-derived correction to the nadir reflectivity to compute "specular" reflectivity (ρ_0) without small scale roughness effects [10], and (2) estimate the average backscatter coefficient (σ_0) within each footprint. Averaging the backscatter coefficient results in σ_0 values in between the high σ_0 of radar-facing slopes and diminished σ_0 of backslopes, thereby eliminating local incidence angle effects. Following the approach in [7], we search for deviations in σ_0, ρ_0 from their respective mean values.

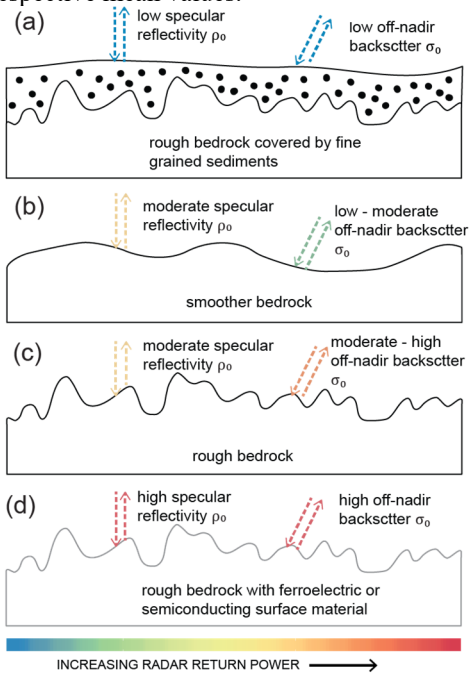

Fig 1. Illustration of how variability in tesserae surfaces impact on Magellan reflectivity and backscatter data.

Tesserae, due to high degree of deformation and consequent high radar-roughness, typically have high SAR backscatter, and moderate nadir reflectivity (Fig 1c). Some regions of tesserae (limited to high altitudes where planetary radius R_p > 6053-6055 km), exhibit high values for off-nadir backscatter and nadir-reflectivity due to the presence of high reflectivity surface materials, which dominate roughness effects (Fig 1d). Locations within tesserae that have lower than average σ_0 represent smoother (at centimeter-scale) surfaces (Fig 1a and b), which could either be due to the presence of fine-grained mantling material, or due to low levels of centimeter-scale deformation. We investigate if the reduction in roughness is due to

mantling or variations in levels of deformation by utilizing nadir reflectivity data. Rocky surfaces mantled by sediments with low dielectric permittivity (Fig 1a) would exhibit lower specular reflectivity relative to less deformed, smoother tessera bedrock (Fig 1b). To avoid biasing mean σ_0 and ρ_0 towards higher values for tessera where high-reflectivity materials are present at high altitudes, we use the elevation thresholds used in [10] to implement this approach separately for high and low altitude regions within each tessera.

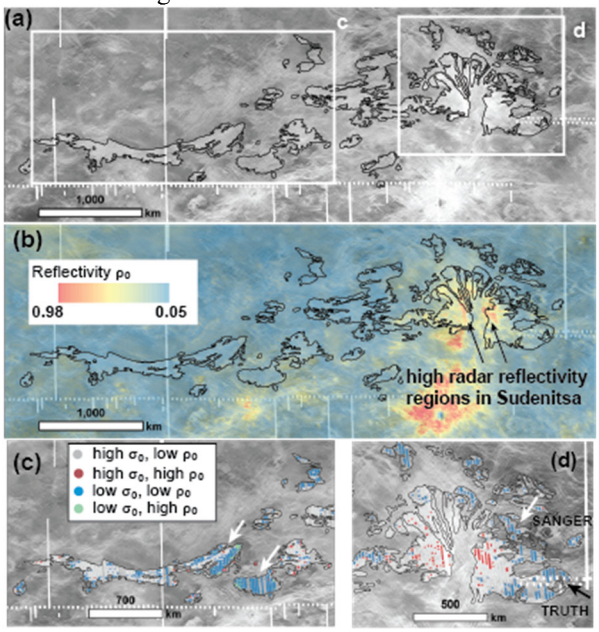

Fig 2. Backscatter and reflectivity variations across Sudenitsa. (a) Magellan SAR backscatter (b) Gridded specular reflectivity derived from Magellan altimetry. (c) western and (d) eastern sections of Sudenitsa with low σ_0 and ρ_0 material (light brown). Low σ_0 regions noted in [7] are indicated by white arrows; newly identified with low σ_0 and ρ_0 in the southeast is indicated by a black arrow.

Results and Discussion: We highlight results from Sudenitsa tessera (Fig. 2), which exhibits both backscatter and reflectivity variations. Elevation within Sudenitsa varies from R_p = ~6048.7 km to ~6058.5 km. Parts of the tessera at altitudes above R_p = 6053 km exhibit high radar reflectivity (Fig 2b), suggested to be caused by the presence of ferroelectric minerals [11]. Previous work has identified SAR-dark fines in the western section, and along the northeastern boundary of Sudenitsa [7]. Our methodology shows similarly low backscatter and lower than average specular reflectivity, supporting existing studies of low-density, fine-grained material in these locations (see Fig 2c and 2d).

We identify an additional region in southeastern Sudenitsa (indicated by a black arrow Fig. 2d), that shows low backscatter and specular reflectivity behavior, in comparison to other parts of the tessera at similar altitudes. This region lies proximal to two large craters: Truth crater (diameter D = 46.1 km), and Sanger crater (D = 83.8 km). Despite having large diameters, these craters do not have visible parabolic ejecta deposits today, suggesting removal of associated parabola deposits via aeolian processes or volcanic resurfacing [12]. Models of crater parabola extents and thickness at the time of emplacement show that the low-backscatter, low-reflectivity region in southeastern Sudenitsa lies within the expected original parabola extent of both Truth and Sanger craters and could have been covered by fine-grained ejecta ranging from few tens of centimeters to more than a meter in thickness [13]. We interpret the low σ_0 and ρ_0 values observed as an indicator of either partial or complete preservation of these sediments within Sudenitsa, similar to sites within tesserae elsewhere on Venus [6,7].

Conclusion and future work: We have presented a methodology for characterizing variability in tessera using two types of Magellan datasets and apply it for identifying locations within the tessera that are smoother either due to mantling or due to lower original cm-scale roughness in the tesserae.. Using Sudenitsa as an example, we confirm previously proposed sites of sediments within the tessera and also identify newer regions that could be mantled by fine grained material.

Future work will involve combined interpretations of these two datasets together, across all tesserae on Venus to identify further inter- and intra-tessera variability in terms of physical properties and composition.

Acknowledgments: This work was supported a Wesleyan internal grant to MSG. Tessera maps were provided by J. Brossier.

References: [1] Ivanov, M. A. & Head, J. W. (1996) JGR, 101, pp. 14861–14908. [2] McKinnon, W.B. et al. (1997) *Venus II*, pp. 969–1014. [3] Strom, R.G. (1994) *JGR:Planets (99)*, pp. 10899–10926. [4] Garvin, J. B. et al. (2022) *PSJ (3),* 117. [5] Beauchamp, P. et al. (2021) *IEEE Aero. Conf. (50100)*, pp. 1-18. [6] Campbell, B. A. et al. (2015) *Icarus (250),* pp. 123-130. [7] Whitten, J. L. and Campbell, B. A. (2016) *Geology (44),* 7. [8] Morgan, H. F. (1994) MGN-V-RDRS-5-DIM-V1.0, NASA PDS. [9] Ford, P. G. (1992). MGN-V-RDRS-5-CDR-ALT/RAD-V1.0, NASA PDS. [10] Pettengill, G. H. et al. (1988) *JGR: Sol. Earth (93)*, B12, pp 14757-15344. [11] Brossier, J. and Gilmore, M. S. (2021) *Icarus (355)*, 114161. [12] Izenberg, N. R. et al. (1994) *GRL (21),* pp. 289–292. [13] Ganey, T. M., et al. (2023) *PSJ.*, in press.